Chapter 6

Application of non-linear system identification

The principles introduced in chapter 5 were implemented into a comprehensive toolbox of NARX related Matlab M-functions (see Appendix F). These functions include non-linear system identification and simulation tools that allow relative easy access to complex mathematical routines capable of modelling severely non-linear MIMO dynamic systems. All applications, NARX and the various modifications thereof, make use of a full parameter set estimation technique based on the orthogonal decomposition method described in Section 5.3.

In general, practical test systems did not warrant the use of the non-linear techniques. NARX techniques did not necessarily render improved simulation results on test systems for which the linear QanTiM techniques failed to accurately simulated system responses. Typical examples of such test systems are listed in Table 6.1.

Table 6.1 Test rigs were NARX did not alleviate problems encountered with QanTiM

No. of axis	Test specimen / configuration	Desired response
7	Commercial vehicle load body [13]	Operational acceleration response
7	Commercial vehicle load body [59]	Operational acceleration response
7	Chassis mounted fuel tank [17]	Operational acceleration response
5	Aircraft engine cradle [12]	Pre-defined flight load spectrum
4	Full vehicle road simulation [24]	Operational acceleration response
3	Heavy vehicle engine assembly [45]	Operational acceleration response
2	Commercial vehicle fuel tank assembly [50]	Operational acceleration response
1	Motorcycle rear wheel simulator (LGI)	Operational strain response

Some test systems did however render improved simulation results with NARX techniques. Furthermore, the NARX technique showed potential as a general modelling tool, capable of accurately modelling highly non-linear dynamic systems. Examples of NARX modelling and simulations are presented for five practical test systems.

6.1. Case study 1: Non-linear elastomeric damper

Elastomeric damper units generally show highly non-linear stiffness characteristics. The static displacement / load relationship of an elastomeric cabin mounting damper used on off-road vehicles is shown in Figure 6.1(a). The damper unit showed severe non-linearity including hystiresis.

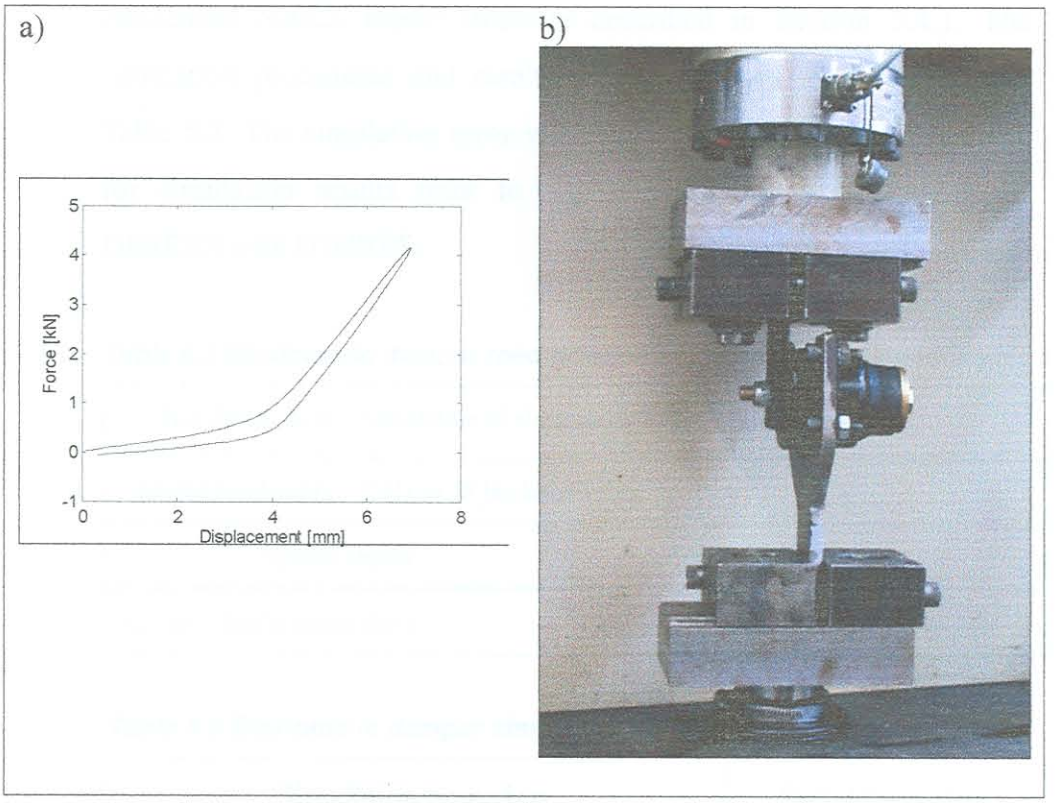

Figure 6.1 Elastomeric damper static stiffness characteristics and test set-up

Two application examples are presented for the elastomeric damper test system shown in Figure 6.1(b):

- Test 1: A road simulation test, reproducing damper load responses measured while travelling through an obstacle on a rough gravel road.
- Test 2: The damper test system is utilised to demonstrate the application of non-linear error signal modelling.

6.1.1. Reconstruction of elastomeric damper field load response

The damper unit was subjected to tests that simulate loads measured whilst negotiating a slow ditch. The dynamic response of the damper unit was simulated using linear QanTiM methods, as well as the condensed NARX model structure described in Section 5.4.1. The simulation procedures and results are summarised in Table 6.2 and Table 6.3. The simulation error values (see Section 5.7) are calculated for simulation results prior to any iteration, i.e. a comparison of DESRES with IT00RES.

Table 6.2 Elastomeric damper road simulation test – System summary

Test description: Simulation of elastomeric damper load response	
Model bandwidth: 0 Hz to 25 Hz Bandwidth	
System Inputs	System Outputs
Actuator displacement drive	Damper load response

Table 6.3 Elastomeric damper simulation results

Simulation procedure	Simulation error
QanTiM 6^{th} order model (inverse)	57 %
NARX 4^{th} order quadratic model (inverse)	24 %

A 6^{th} order QanTiM model showed the best simulation results, with no further improvement in accuracy with an increase in model order. The 6^{th} order QanTiM model made use of 13 polynomial terms. The full parameter set NARX description made use of 54 terms for the 4^{th} order quadratic model. The results for both model types are shown in Figure 6.2.

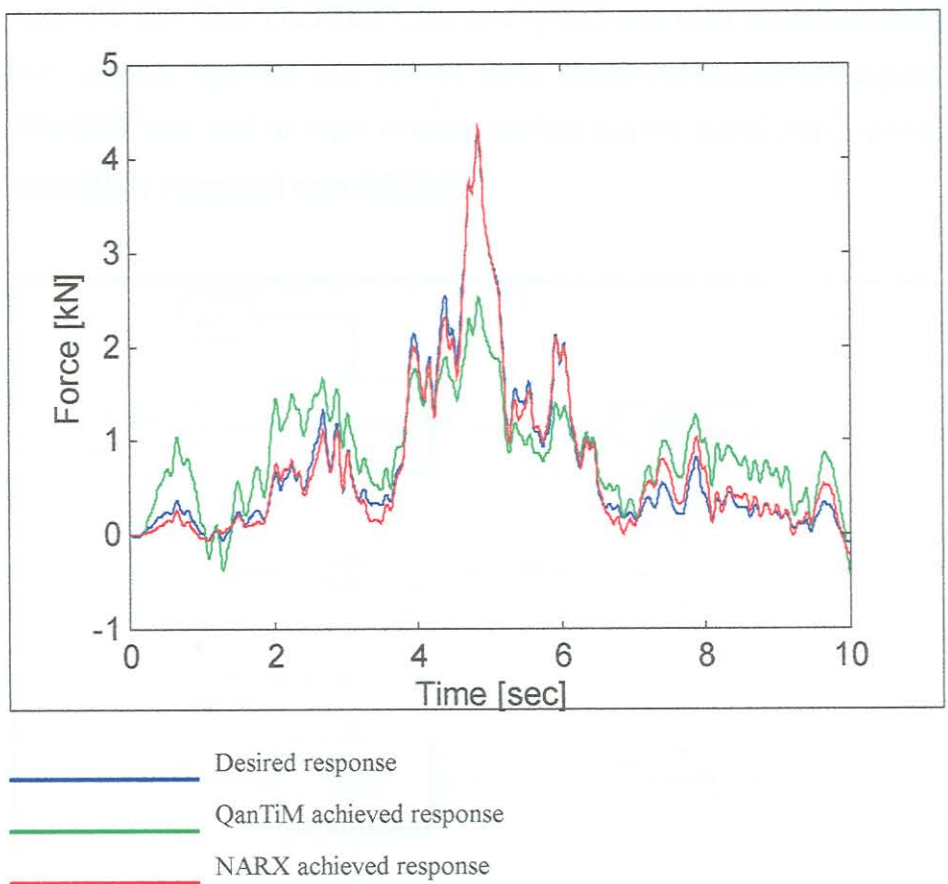

Figure 6.2 QanTiM vs. NARX simulation results

The NARX simulation technique shows clear advantage over the linear QanTiM technique. QanTiM failed to accurately model, and subsequently simulate the severe non-linear behaviour of the elastomeric damper unit. Simulations conducted with NARX show good reconstruction of load response over a broad amplitude range.

6.1.2. Non-linear error signal modelling of an elastomeric damper

The elastomeric damper test system presented in Figure 6.1 is utilised to demonstrate the potential of the non-linear error signal modelling technique presented in Section 5.5.4. The test system was excited with a random drive signal (SIMDRV) and the subsequent pseudo desired response recorded (DESRES). The test system was then identified using both normal QanTiM and NARX error signal modelling techniques. SIMDRV was used as input to these models and the simulated response (SIMRES) compared with DESRES.

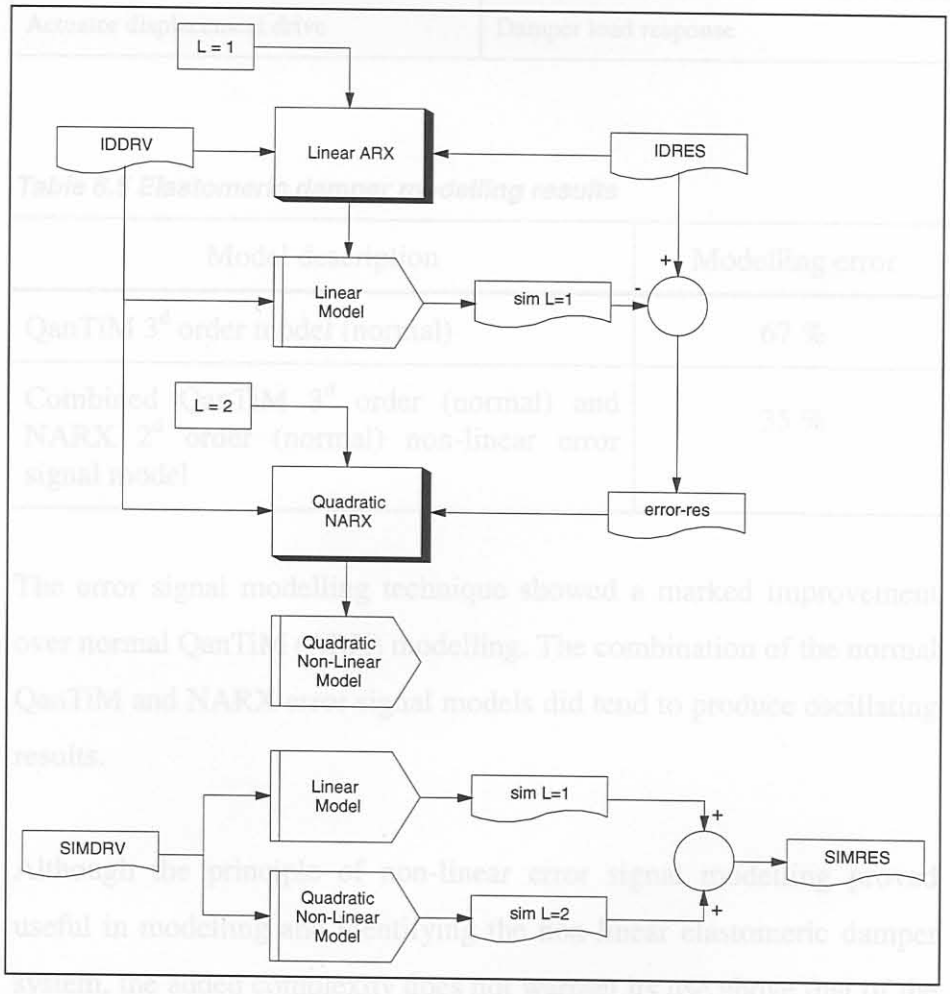

Figure 6.3 Quadratic non-linear error signal modelling

A 3^{d} order linear normal QanTiM model was used to characterise the damper unit's linear response. A 2^{d} order quadratic model was then used to model the error signal. No cubic model was used. The non-linear error signal modelling process is shown in Figure 6.3. The modelling results are shown in Figure 6.4.

Table 6.4 Elastomeric damper modelling – System summary

Test description:	Identification and modelling of elastomeric damper load response
Model bandwidth:	0 Hz to 25 Hz
System Inputs	System Outputs
Actuator displacement drive	Damper load response

Table 6.5 Elastomeric damper modelling results

Model description	Modelling error
QanTiM 3^{d} order model (normal)	67 %
Combined QanTiM 3^{d} order (normal) and NARX 2^{d} order (normal) non-linear error signal model	35 %

The error signal modelling technique showed a marked improvement over normal QanTiM (ARX) modelling. The combination of the normal QanTiM and NARX error signal models did tend to produce oscillating results.

Although the principle of non-linear error signal modelling proved useful in modelling and identifying the non-linear elastomeric damper system, the added complexity does not warrant its use above that of the condensed NARX formulation.

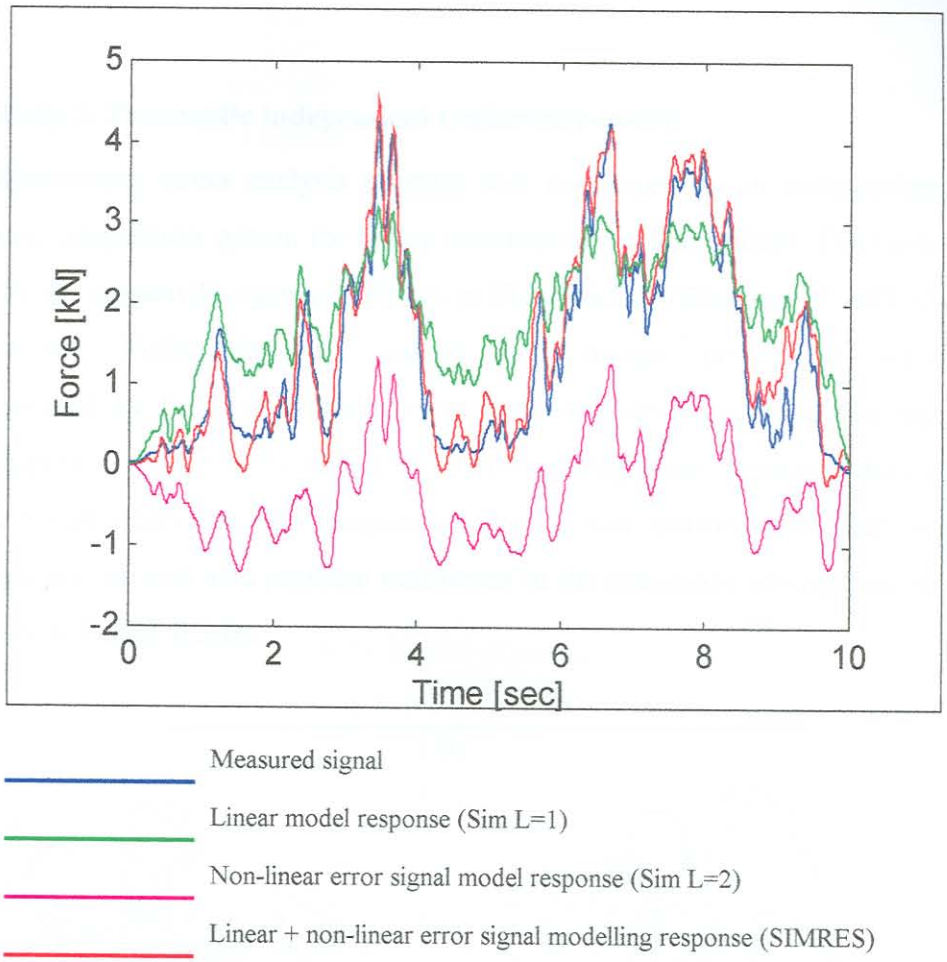

Figure 6.4 Non-linear error signal modelling response for an elastomeric damper

6.2. Case study 2: Pneumatic independent trailer suspension

A comprehensive stress analysis exercise was conducted on an independent pneumatic suspension system for heavy commercial vehicle trailers. The basic layout of the suspension system is shown in Figure 6.5(a) (Courtesy of ASTAS Automotive). Finite element analysis and design procedures were complimented by full-scale simulation testing on a servo-hydraulic test rig. Strain inputs to both the FEA and simulation testing were measured during normal trailer operation. The suspension system was instrumented with 10 strain gauges, as well as a pressure transducer in the pneumatic spring unit, as indicated in Figure 6.5(b).

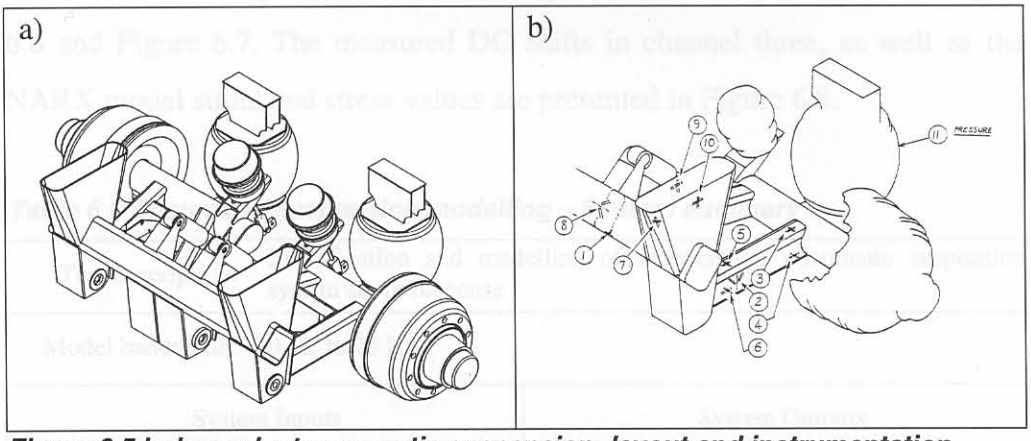

Figure 6.5 Independent pneumatic suspension: layout and instrumentation

The most critical stress area was found to be on the top flange of the suspension swing arm, in the region of strain channel three. While driving with an over-laden trailer on rough road conditions, a substantial DC shift was recorded for channel three (see Figure 6.8 – measured data). Such a large DC shift could typically indicate plastic deformation of the component. Alternatively, instrumentation errors, or so-called welding shakedown could cause the DC shift. Due to the critical location of channel three, it was of paramount importance to determine whether plastic deformation did indeed occur in the suspension swing arm.

Part of the investigation into the possible plastic deformation involved modelling strain (or approximate stress) responses with NARX techniques. A dynamic model was identified between the pressure response in the pneumatic spring unit, and the strain response at channel three. The dynamic model was identified and validated on Sections of true data, and subsequently used to predict the suspect strain response at channel three as a function of the pressure in the pneumatic spring.

Linear normal QanTiM models failed to model strain response as a function of pneumatic spring pressure, whereas NARX models provided accurate results (see Table 6.6 through Table 6.7). Model identification and validation were conducted with the pressure and strain response time histories shown in Figure 6.6 and Figure 6.7. The measured DC shifts in channel three, as well as the NARX model simulated stress values are presented in Figure 6.8.

Table 6.6 Pneumatic suspension modelling – System summary

Test description:	Identification and modelling of independent pneumatic suspension system strain response
Model bandwidth:	0 Hz to 25 Hz
System Inputs	System Outputs
Pneumatic spring unit pressure response	Channel three strain response

Table 6.7 Pneumatic suspension modelling results

Model description	Modelling error
QanTiM 5^{th} order model (normal)	95 %
NARX 3^{d} order quadratic model (normal)	34 %

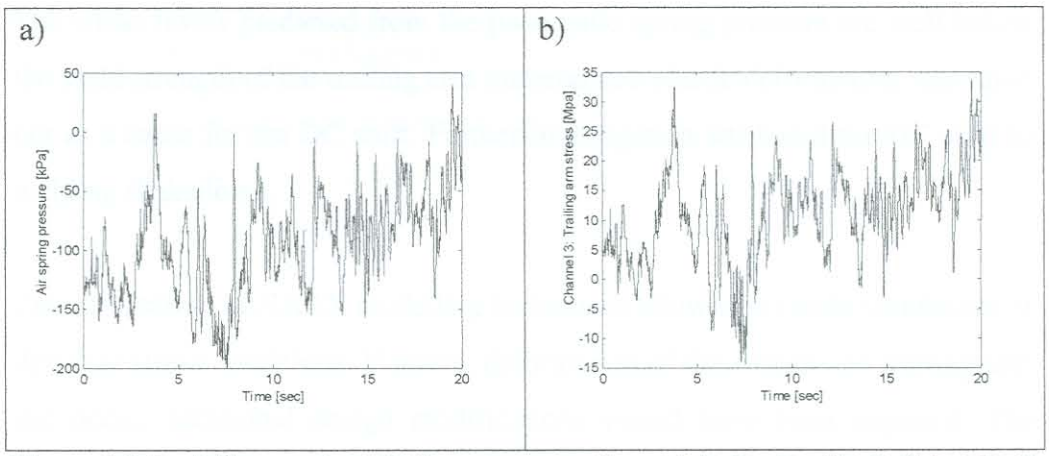

Figure 6.6 Modelling and validation response time histories for the independent suspension system

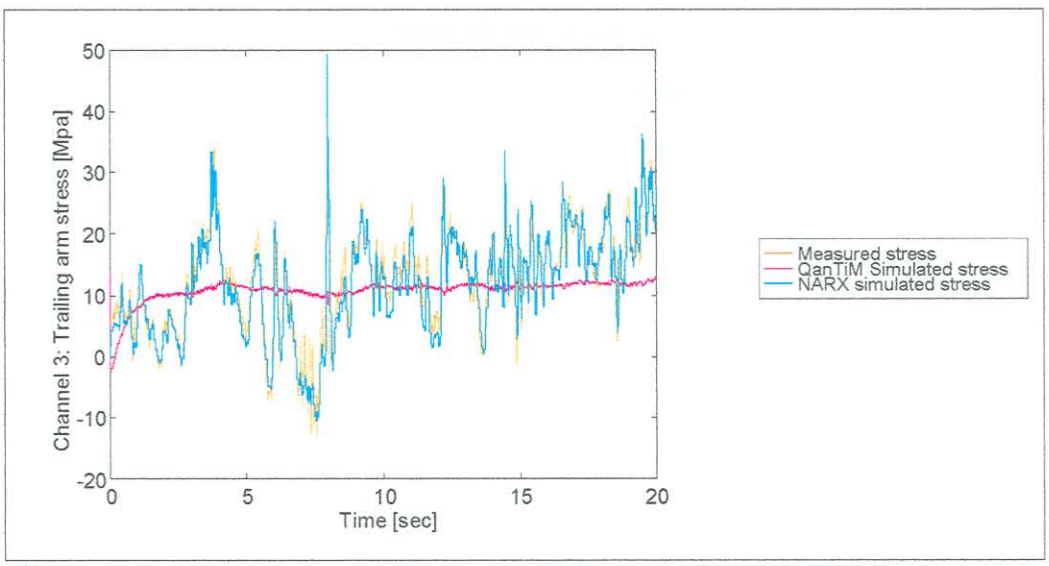

Figure 6.7 Linear vs. non-linear modelling results for the independent suspension system

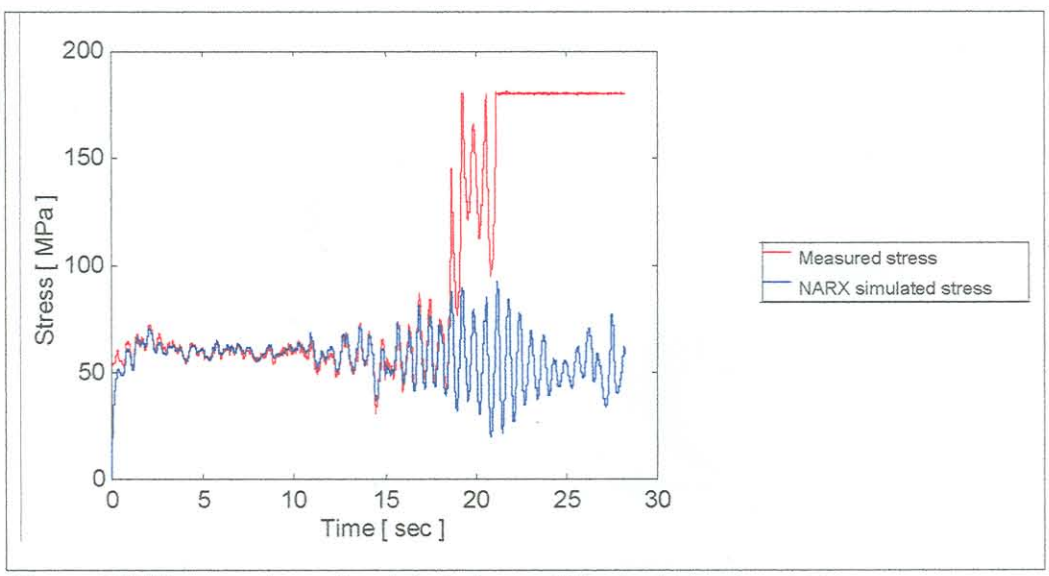

Figure 6.8 Measured vs. simulated channel three stress response

The stress levels predicted from the pneumatic spring pressure are well below the yield strength of the trailing arm material and plastic deformation was ruled out as a cause for the DC shift. Further investigation attributed the DC shift to welding shakedown.

The application of NARX modelling techniques allowed accurate simulation of dynamic stress conditions. If plastic deformation of the suspension trailing arm did occur, additional design modifications would have been required. The simulated stress results obtained with the NARX model averted any such modifications.

6.3. Case study 3: Light truck front suspension

Two examples are presented where split spectra linear-non-linear modelling techniques were used to describe the dynamic behaviour of systems too complex for linear normal QanTiM modelling. The two applications further show the capability of the condensed NARX model formulation to describe non-square systems (number of inputs ≠ number of outputs). Both application examples are concerned with modelling, and subsequently simulating, suspension system stresses as a function of wheel loads for the front suspension of a light truck [16] (courtesy of GM corporation, Pontiac, Michigan). The front suspension of the truck was extensively instrumented with strain gauges. The wheels were instrumented to measure input loads to the suspension system. The first example models the longitudinal force in the upper suspension ball joint as a function of the wheel input loads. The second example models forces in, and displacements of the upper and lower suspension control arms as a function of the wheel input loads. A schematic representation of the suspension system is shown in Figure 6.9.

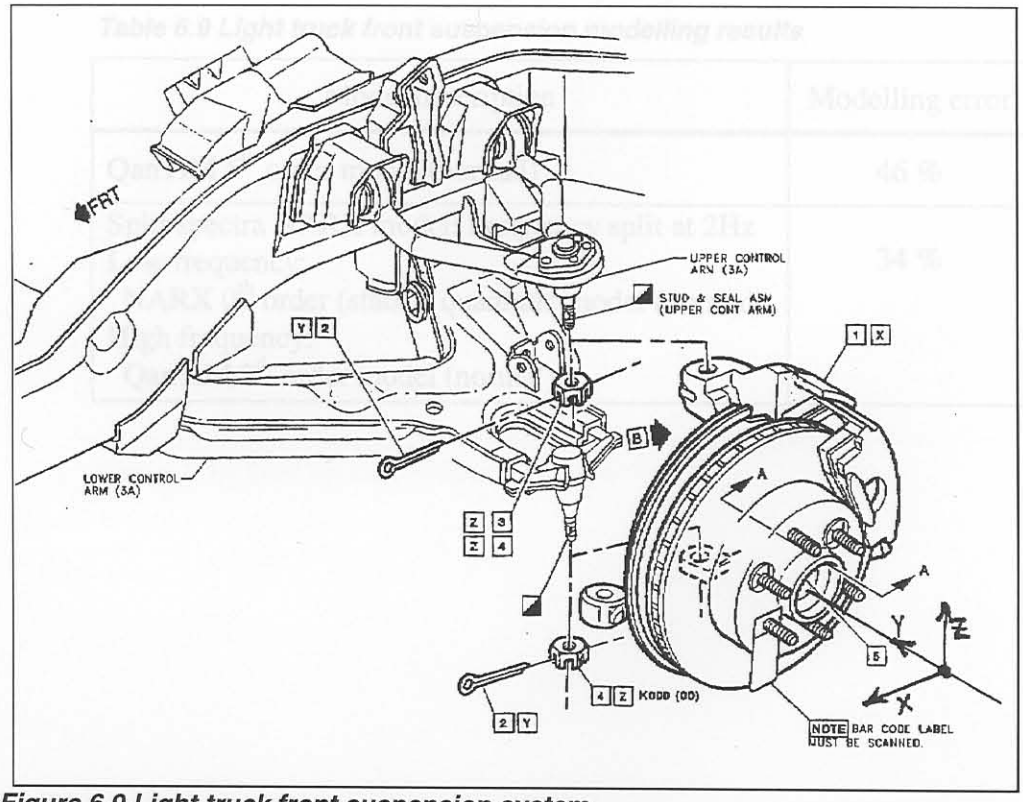

Figure 6.9 Light truck front suspension system

6.3.1. Light truck suspension: Wheel ⇒ upper ball joint forces

The upper ball joint longitudinal reactions are modelled to wheel input loads. This MISO system illustrates the effect of the non-linear terms, and its improved accuracy achieved over linear modelling.

Table 6.8 Light truck front suspension modelling – System summary

Test description:	Identification and modelling of light truck front suspension system strain response
Model bandwidth:	0 Hz to 25 Hz
System Inputs	System Outputs
• Spindle longitudinal force X • Spindle lateral force Y • Spindle vertical force Z • Moment about X axis • Moment about Y axis • Moment about Z axis	• Longitudinal forces at the upper suspension ball joint

Table 6.9 Light truck front suspension modelling results

Model description	Modelling error
QanTiM 5th order model (normal)	46 %
Split spectra NARX model: Frequency split at 2Hz Low frequency: NARX 0th order (static), quadratic model (normal) High frequency: QanTiM 2^{d} order model (normal)	34 %

Both drive and response data are split using a 4th order digital filter. A static quadratic model is used to describe the low frequency part, whereas a second order linear model is used for the high frequency part. The two frequency ranges are modelled and simulated independently, the responses are summed to obtain simulation over the whole spectrum.

The measured and simulated response signals for both the low and high frequency ranges are shown in Figure 6.10. Note that the low frequency model produced a near perfect fit (in the graph below, the two lines are plotted on one another), but the high frequency model is less accurate.

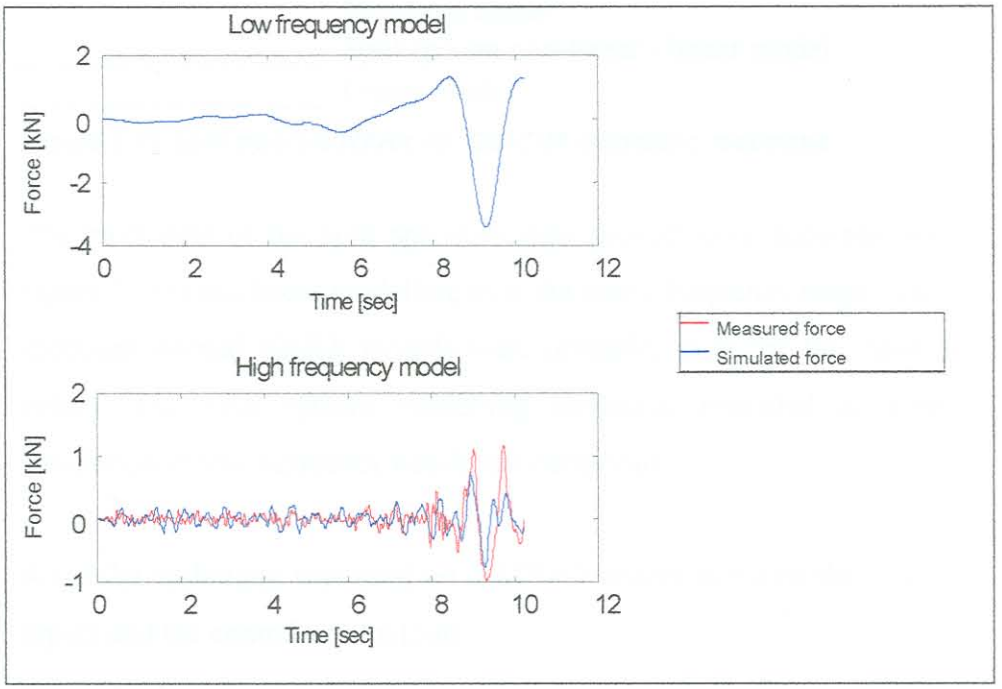

Figure 6.10 Split spectra model response

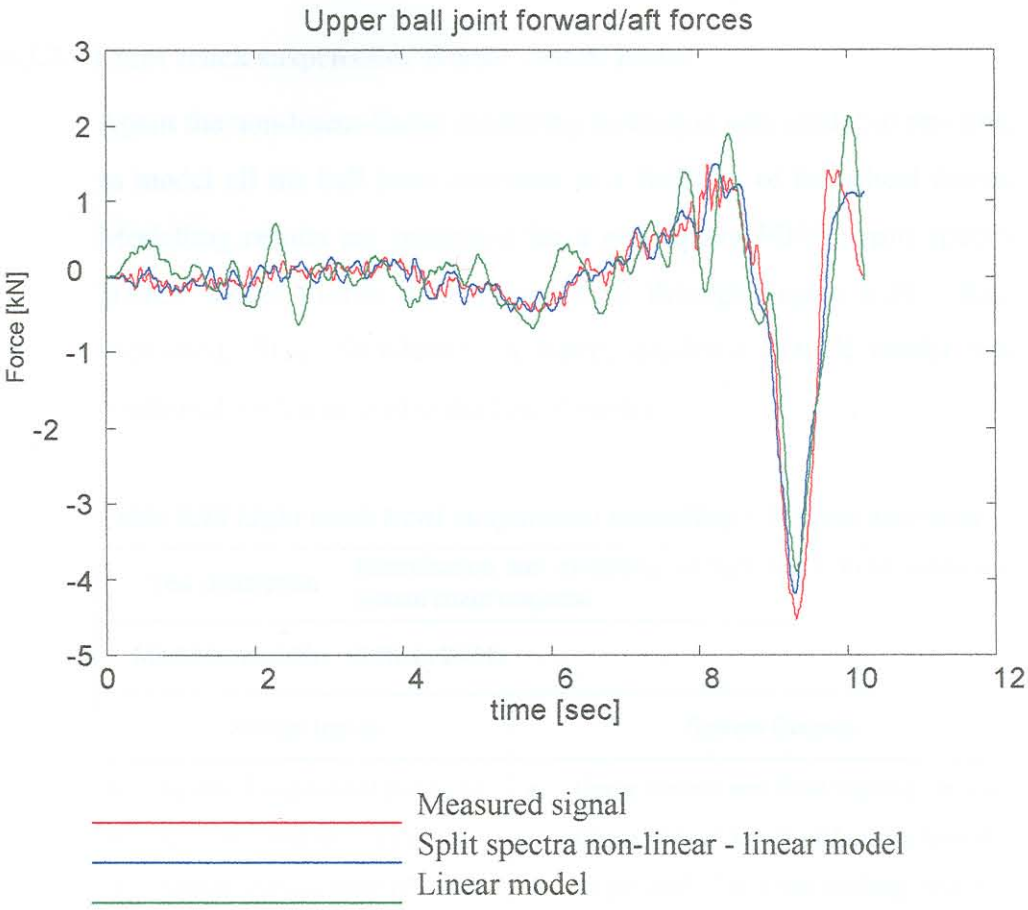

Figure 6.11 Split spectra NARX vs. QanTiM modelling response

The modelling of the split spectrum data proved more accurate (see Figure 6.11) than linear modelling over the entire frequency range. Full spectrum normal NARX models were unstable, even for low model orders. The split spectra modelling technique provided accurate simulation of low frequency non-linear behaviour

A similar technique was used on a MIMO system between the wheel inputs and the control arm outputs.

6.3.2. Light truck suspension: Wheel ⇒ ball joints

Again the non-linear-linear modelling technique was used, but this time to model all the ball joint reactions as a function of the wheel forces. Modelling results are presented for a non-square MIMO split spectra NARX model (Table 6.10, Figure 6.12 through Figure 6.20 - Red: Measured, Blue: Simulated). A static, quadratic NARX model was combined with a second order linear model.

Table 6.10 Light truck front suspension modelling – System summary

Test description:	Identification and modelling of light truck front suspension system strain response
Model bandwidth:	0 Hz to 25 Hz
System Inputs	System Outputs
• Spindle Longitudinal force (X) • Spindle lateral force (Y) • Spindle vertical force (Z) • Moment about X axis • Moment about Y axis • Moment about Z axis	• Upper control arm front bushing vertical • Upper control arm front bushing lateral • Upper control arm rear bushing vertical • Upper control arm rear bushing lateral • Lower control arm front bushing vertical • Lower control arm front bushing lateral • Lower control arm rear bushing vertical • Lower control arm rear bushing lateral • Lower control arm angular displacement

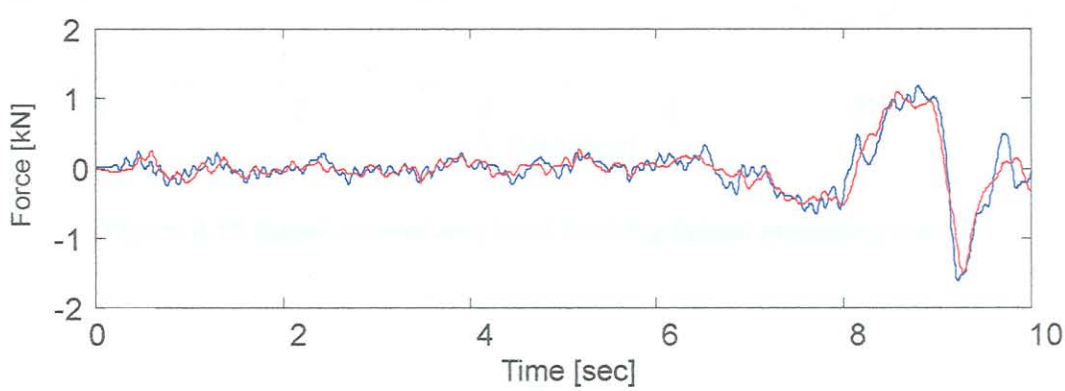

Figure 6.12 Upper control arm front bushing vertical modelling results

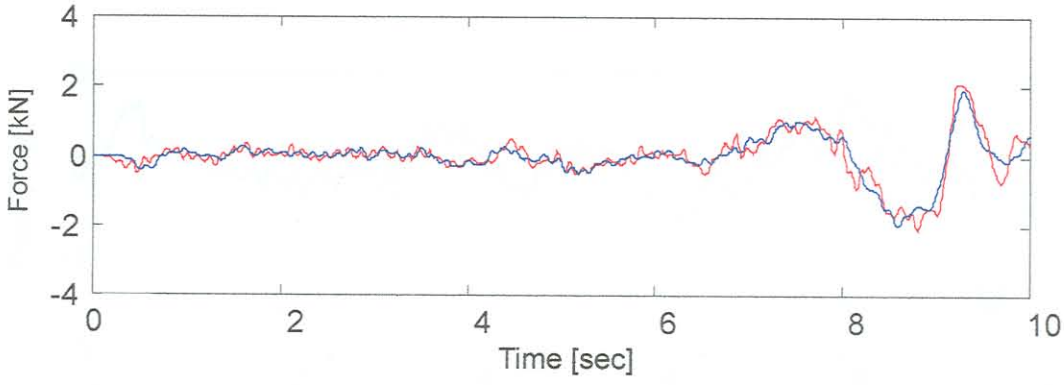

Figure 6.13 Upper control arm front bushing lateral modelling results

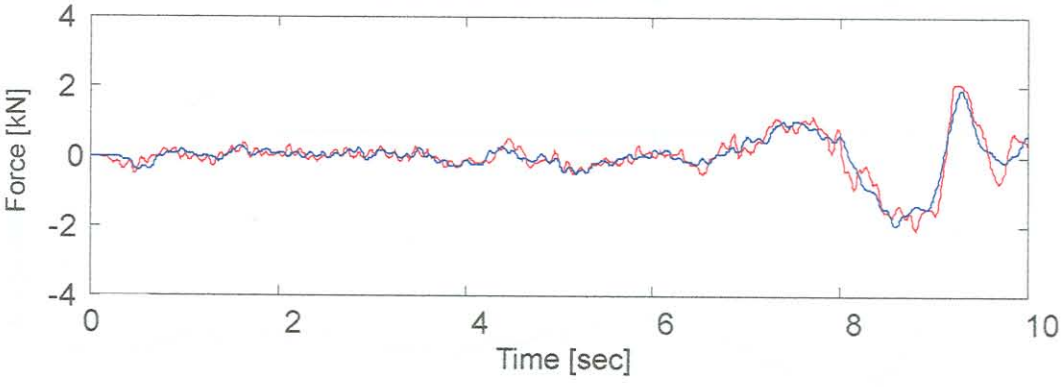

Figure 6.14 Upper control arm rear bushing vertical modelling results

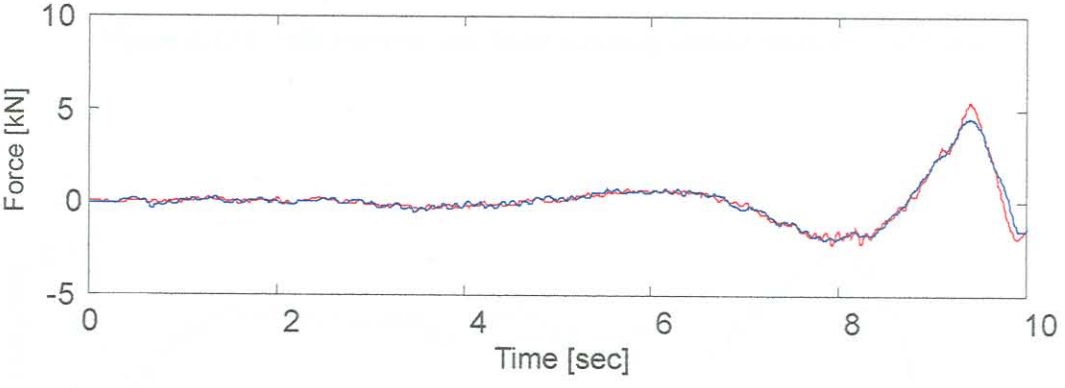

Figure 6.15 Upper control arm front bushing lateral modelling results

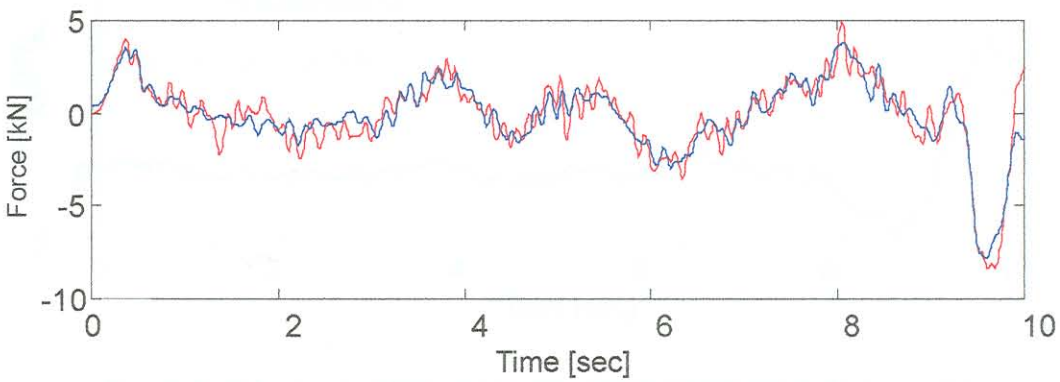

Figure 6.16 Lower control arm front bushing vertical modelling results

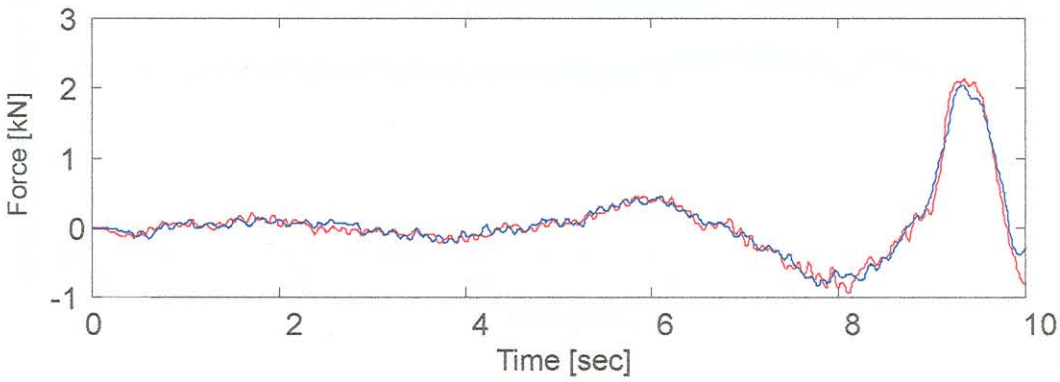

Figure 6.17 Lower control arm front bushing lateral modelling results

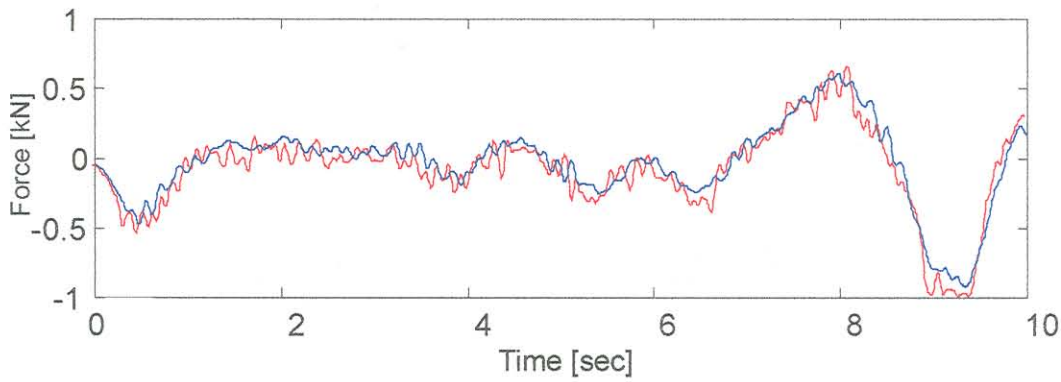

Figure 6.18 Lower control arm rear bushing vertical modelling results

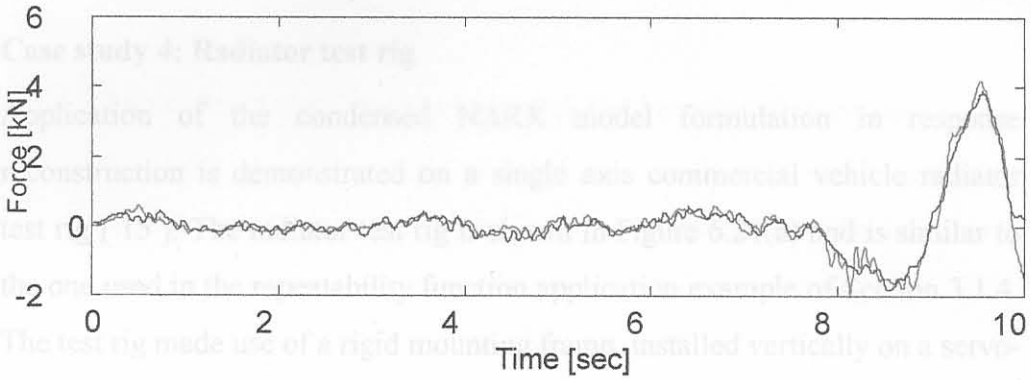

Figure 6.19 Lower control arm rear bushing lateral modelling results

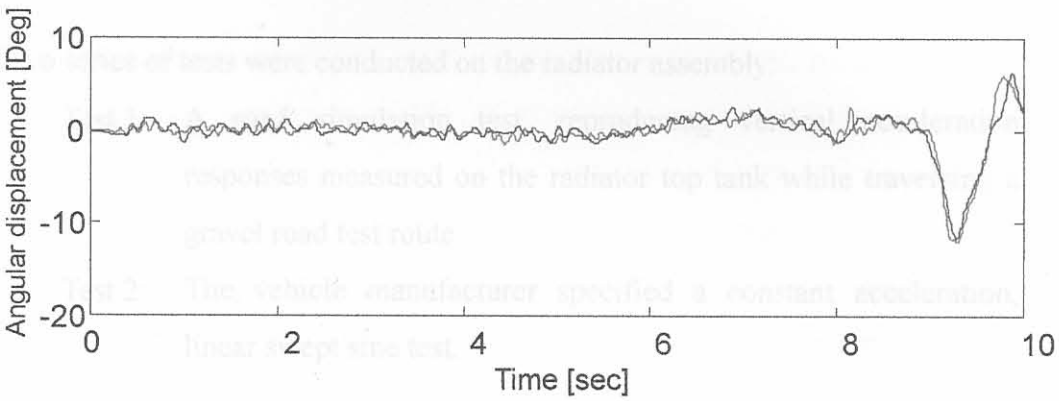

Figure 6.20 Lower control arm angular displacement modelling results

6.4. Case study 4: Radiator test rig

Application of the condensed NARX model formulation in response reconstruction is demonstrated on a single axis commercial vehicle radiator test rig [15]. The radiator test rig is shown in Figure 6.21(a) and is similar to the one used in the repeatability function application example of Section 3.1.4. The test rig made use of a rigid mounting frame, installed vertically on a servo-hydraulic actuator. Mounting pins on the top and bottom radiator tanks fitted into doughnut shaped rubber mounts. These rubber mounts were fitted to the rigid mounting frame as per normal vehicle installation.

Two series of tests were conducted on the radiator assembly:

- Test 1: A road simulation test, reproducing vertical acceleration responses measured on the radiator top tank while traversing a gravel road test route.
- Test 2: The vehicle manufacturer specified a constant acceleration, linear swept sine test.

a) b)

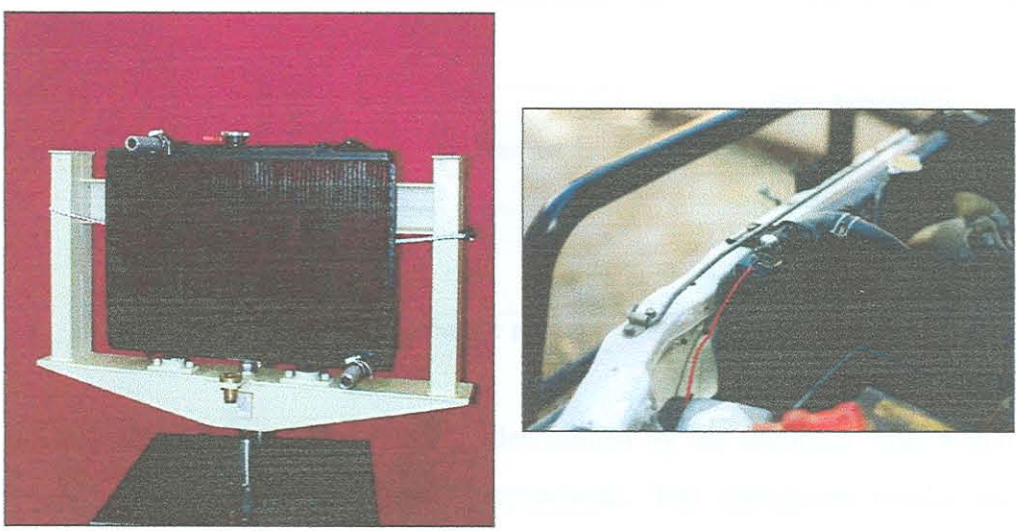

Figure 6.21 Radiator test rig

6.4.1. Reconstruction of radiator top tank field acceleration response

Structural durability tests required the field acceleration response, recorded on the radiator top tank, to be reproduced in the laboratory. Figure 6.21 (b) shows an accelerometer applied to the top tank of the test vehicle's radiator for field measurements. An additional accelerometer was applied to the vehicle chassis, centred below the radiator. Field responses were recorded while travelling on a gravel road test route.

Results are presented for three simulation exercises, namely a linear QanTiM simulation, a NARX simulation and a non-square NARX simulation. The non-square simulation utilises both the acceleration response channels to predict the actuator drive signals. The non-square dynamic system is shown schematically in Figure 6.22. The use of a second response transducer serves as an aid to improve top tank acceleration simulation.

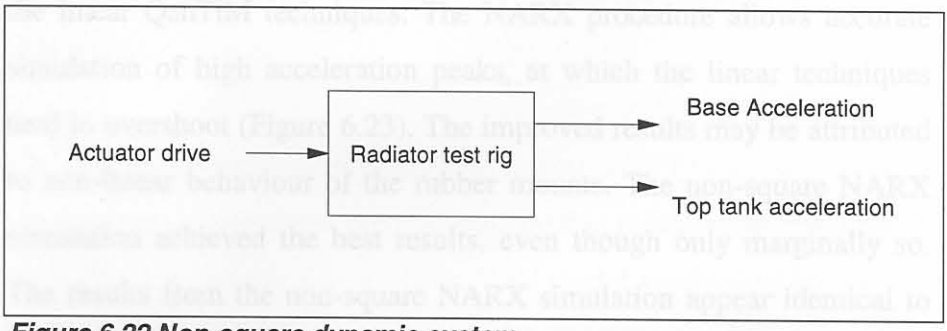

Figure 6.22 Non-square dynamic system

The accuracy of simulation is determined by the accuracy with which the top tank acceleration is reproduced. The simulation results are presented in Table 6.12. The simulation error values (see Section 5.7) are calculated for simulation results prior to any iteration, i.e. a comparison of DESRES with IT00RES.

Table 6.11 Radiator road simulation test - System summary

Test description: Simulation of radiator acceleration response	
Model bandwidth: 2 Hz to 30 Hz	
System Inputs	System Outputs
• Actuator displacement drive	• Radiator top tank acceleration • Radiator base acceleration (only for non-square simulation)

Table 6.12 Radiator simulation results

Simulation procedure	Simulation error
QanTiM 6th order model (inverse)	35 %
NARX 6th order quadratic model (inverse)	16 %
Non-square NARX 6th order quadratic model (inverse)	14 % (base acceleration: 12 %)

The NARX simulation procedure produced results superior to that of the linear QanTiM techniques. The NARX procedure allows accurate simulation of high acceleration peaks, at which the linear techniques tend to overshoot (Figure 6.23). The improved results may be attributed to non-linear behaviour of the rubber mounts. The non-square NARX simulation achieved the best results, even though only marginally so. The results from the non-square NARX simulation appear identical to that of the SISO NARX and are not shown.

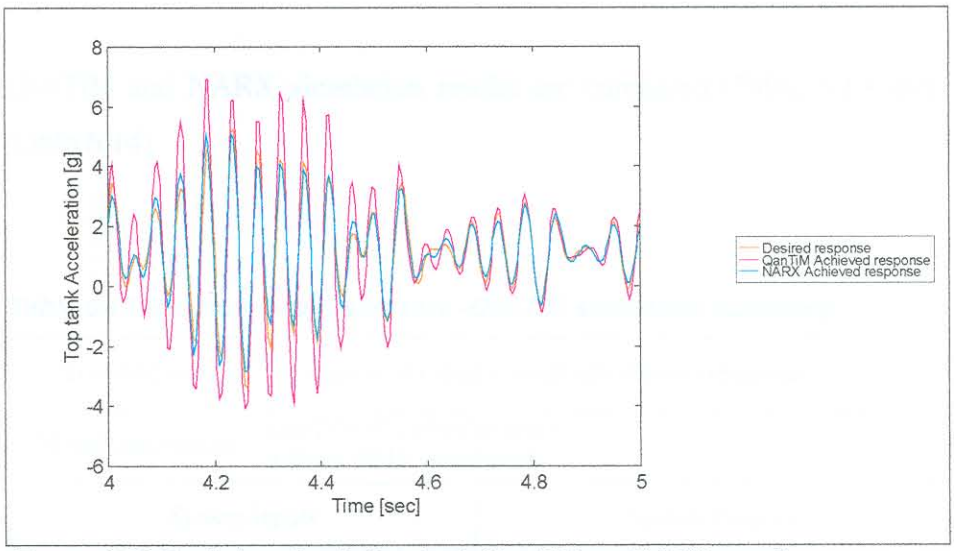

Figure 6.23 Radiator simulation test, QanTiM vs. NARX results

6.4.2. Radiator sine sweep tests

The second phase of the radiator test series consisted of a constant acceleration swept sine test. The test prescribed a 10 Hz to 50 Hz swept sine response at a constant acceleration amplitude of 1.5 g, measured at the base of the mounting frame. Due to inherent system resonance, the prescribed test response fell beyond the capabilities of the actuator's servo control system. A response reconstruction technique was subsequently employed, with the 1.5 g swept sine as desired response (DESRES).

The aim of the simulation procedure was to identify a model between the actuator displacement drive signal and the acceleration response on the radiator mounting frame's base. This model would then be used to calculate actuator drive signals, which compensate for the system resonance, resulting in the desired test response. It is known that QanTiM has difficulty simulating over areas of resonance [45][50]. This application will indicate whether the NARX techniques improve simulation results over areas of resonance.

QanTiM and NARX simulation results are compared (Table 6.13 and Table 6.14)

Table 6.13 Radiator swept sine test –QanTiM simulation summary

Test description:	Simulation of radiator swept sine desired response
Model description:	QanTiM 9th order (inverse) 8 Hz to 60 Hz Bandwidth
System Inputs	System Outputs
Actuator displacement drive	Radiator base acceleration

Table 6.14 Radiator swept sine test - NARX simulation summary

Test description:	Simulation of radiator swept sine desired response
Model description:	NARX 6th order quadratic (inverse) 8 Hz to 60 Hz Bandwidth
System Inputs	System Outputs
Actuator displacement drive	Radiator base acceleration

The PSD graphs of QanTiM and NARX simulation results (IT00RES) are presented in Figure 6.24. The graphs show the constant PSD amplitude of the desired response, and the achieved resonant for both QanTiM and NARX responses. It is important to note that the effects of resonance appear worsened in the NARX simulation. The best results were achieved with extensive iteration of QanTiM simulation results, as shown in Figure 6.25. Small iteration gain factors were used throughout the iteration process, but even this approach did not relieve the resonance problems.

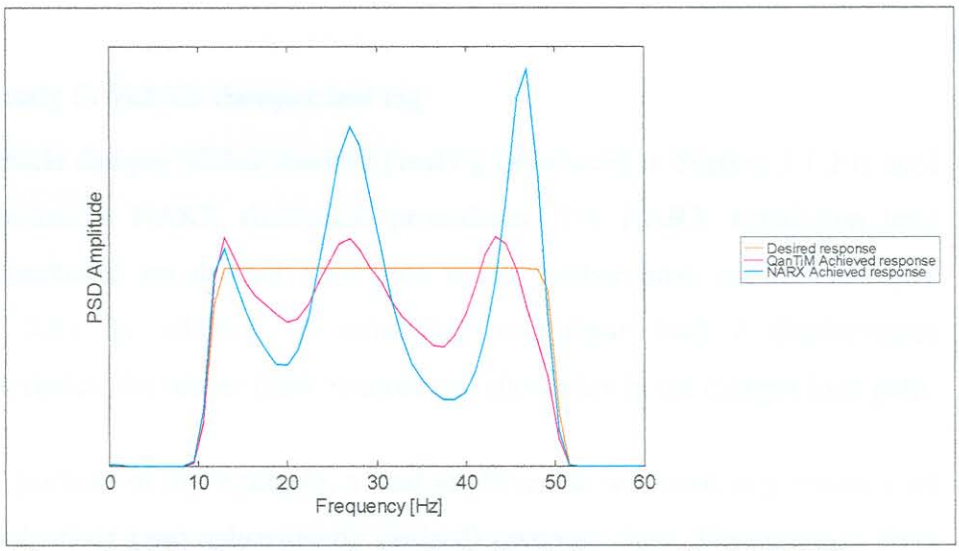

Figure 6.24 Radiator swept sine test simulation results (IT00RES)

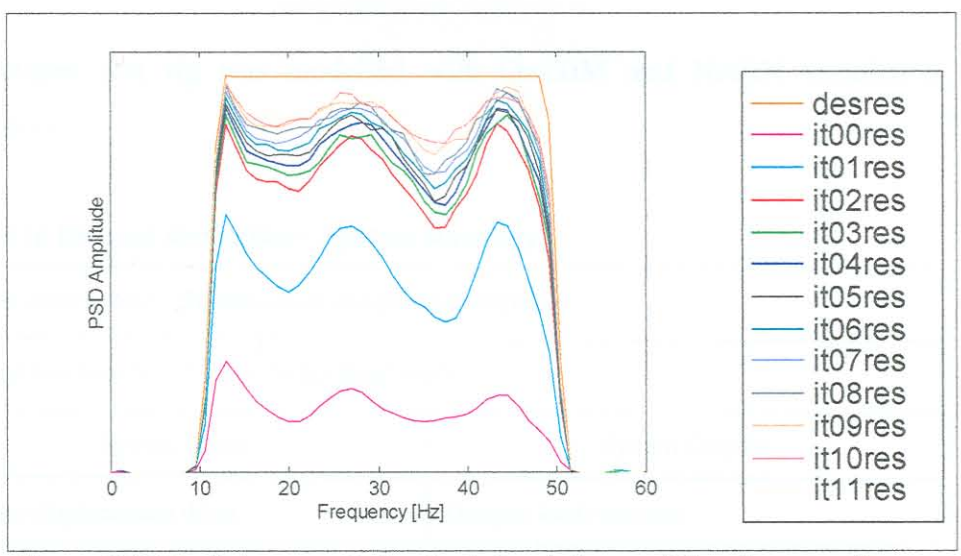

Figure 6.25 Radiator swept sine test simulation and iteration results

6.5. Case study 5: Vehicle damper test rig

The vehicle damper (shock absorber) test rig introduced in Section 3.1.2 is used to demonstrate NARX simulation procedures. The NARX simulation tests were conducted on damper units that utilise rubber bush connections (see Figure 3.3). In addition to exhibiting non-linear load / displacement characteristics, the rubber bush connections allow play in the damper load path.

For the purpose of this example, a random drive file was used to generate a set of pseudo field (and subsequently desired) response data. This random drive file will be referred to as DESDRV, and the subsequent response as DESRES.

The damper test rig was modelled with QanTiM and NARX simulation procedures.

Table 6.15 Damper simulation - System summary

Test description: Simulation of damper load response	
Model bandwidth: 0 Hz to 10 Hz Bandwidth	
System Inputs	System Outputs
Actuator displacement drive	Damper load response

Table 6.16 Damper simulation results

Simulation procedure	Simulation error
QanTiM 4th order model (inverse) IT00RES	27 %
QanTiM 4th order model (inverse) IT05RES	17 %
NARX 4th order cubic model (inverse) IT00RES	18 %

NARX simulation results surpassed linear results achieved with QanTiM. Iteration of the QanTiM results improved on the NARX achievement and produced the best simulation.

Both the QanTiM and NARX techniques rendered good simulation results, i.e. good response reconstruction. Good response reconstruction intuitively implies good reconstruction of system inputs. Thus if FINRES is equal to DESRES, then FINDRV should intuitively be equal to DESDRV. For the damper test rig however, the final drive displays no similarity to the drive used to create the desired response, i.e. FINDRV is not equal to DESDRV. Figure 6.26 compares DESDRV with the NARX (IT00DRV) and QanTiM (IT05DRV) simulation drive files. The corresponding response files are compared in Figure 6.27

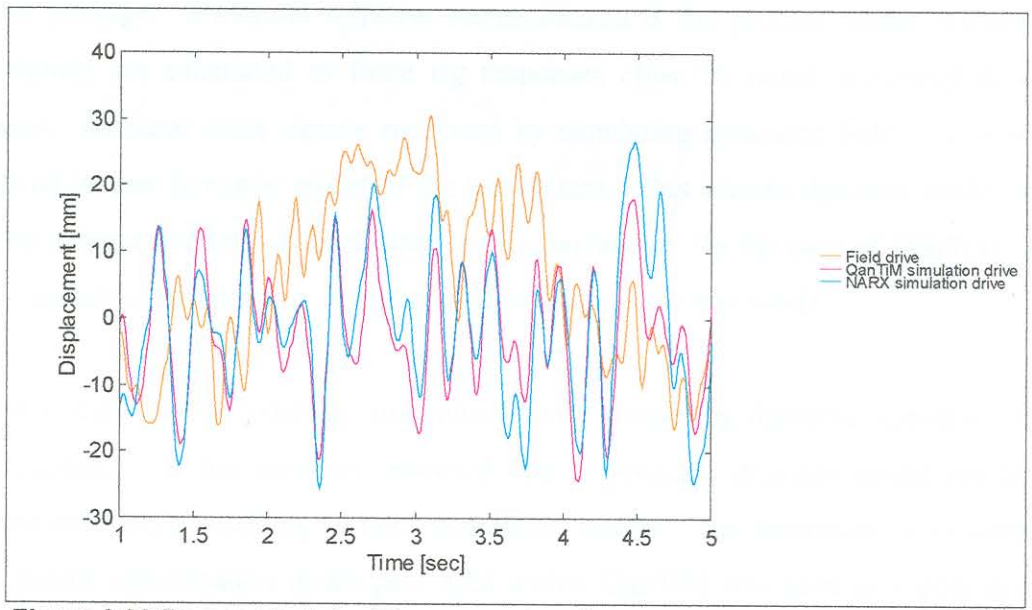

Figure 6.26 Damper test rig drive reconstruction

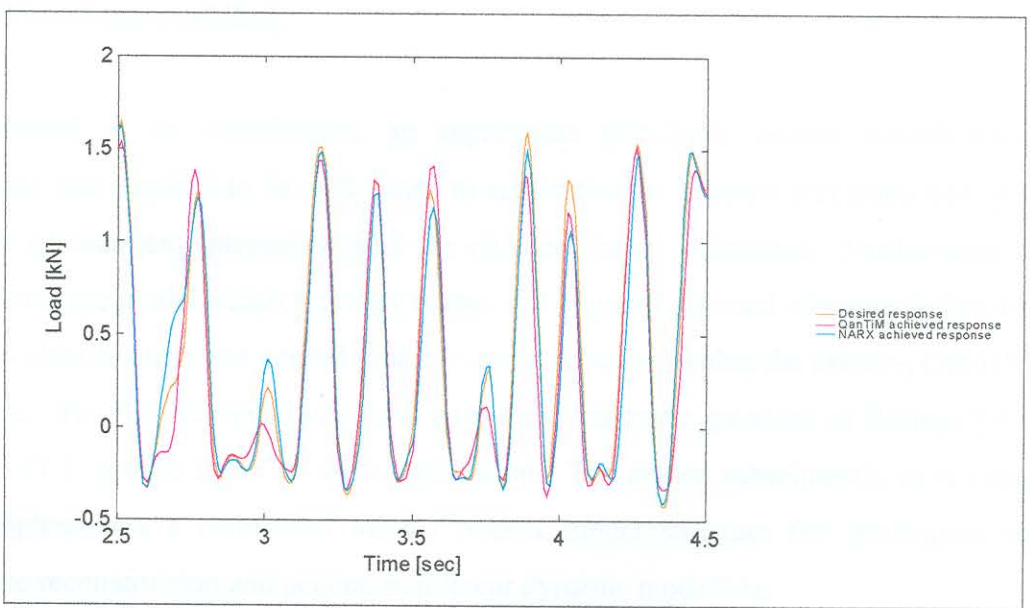

Figure 6.27 Damper test rig response reconstruction